THE JOURNAL OF CHEMICAL PHYSICS **128**, 064509 (2008)

Temperature dependence of the electrical conductivity of imidazolium ionic liquids

Jan Leys,[a] Michael Wübbenhorst, Chirukandath Preethy Menon, Ravindran Rajesh, Jan Thoen, and Christ Glorieux
Laboratorium voor Akoestiek en Thermische Fysica, Departement Natuurkunde en Sterrenkunde, Katholieke Universiteit Leuven, Celestijnenlaan 200D, bus 2416, 3001 Leuven, Belgium

Peter Nockemann, Ben Thijs, and Koen Binnemans
Laboratorium voor Coördinatiechemie, Afdeling Moleculair Design en Synthese, Departement Chemie, Katholieke Universiteit Leuven, Celestijnenlaan 200F, bus 2404, 3001 Leuven, Belgium

Stéphane Longuemart
Laboratoire de Thermophysique de la Matière Condensée (UMR CNRS 8024), Université du Littoral Côte d'Opale, 145 Avenue M. Schumann, F-59140 Dunkerque, France

(Received 12 September 2007; accepted 29 November 2007; published online 14 February 2008)

The electrical conductivities of 1-alkyl-3-methylimidazolium tetrafluoroborate ionic liquids and of 1-hexyl-3-methylimidazolium ionic liquids with different anions were determined in the temperature range between 123 and 393 K on the basis of dielectric measurements in the frequency range from 1 to 10^7 Hz. Most of the ionic liquids form a glass and the conductivity values obey the Vogel-Fulcher-Tammann equation. The glass transition temperatures are increasing with increasing length of the alkyl chain. The fragility is weakly dependent on the alkyl chain length but is highly sensitive to the structure of the anion. © *2008 American Institute of Physics*.

[DOI: 10.1063/1.2827462]

I. INTRODUCTION

Ionic liquids (ILs) have been in recent years the subject of growing research activities because of their interesting physical properties (high electrical conductivity and very low vapor pressure) and their potential as designer solvents for catalytic and chemical applications.[1–4] By definition, ionic liquids are organic salts with a melting temperature below 100 °C. They have a strong tendency to form supercooled melts. The polarity, dielectric constant, electrochemical window, and electrical conductivity are important physical properties which determine whether an ionic liquid is suitable for a given application.

Some classes of ionic liquids are good glass formers. On cooling, the supercooled melt has no tendency to crystallize, but rather it vitrifies. Since ionic liquids exhibit a rich structural variety, a systematic study of the relation between glass formation and molecular structure may improve our understanding of the complex mechanism of glass formation in molecular compounds.

Systematic series of ionic liquids have been synthesized and studied in the past. Examples of such work include Ref. 5, in which a series of 1-butyl-3-methylimidazolium ionic liquids with different fluorinated anions is studied, and a broad range of physical properties have been studied. However, the measurements, except for differential scanning calorimetry (DSC), did not extend below −10 °C, thus far above the glass transition region. The same authors also investigated the influence of the length of the alkyl chain in a series of 1-alkyl-3-methylimidazolium bis(trifluoromethylsulfonyl)imide ionic liquids, under the same experimental circumstances.[6] Conductivity data for a number of 1-alkyl-3-methylimidazolium tetrafluoroborates that extend to somewhat lower temperatures (−20 °C) have been reported.[7] Vogel-Fulcher-Tammann (VFT) parameters have been extracted from these data. Another extensive study of the glass-forming behavior of ionic liquids was given by Xu *et al.*,[8] who compared conductivity and viscosity data and discussed the glass transition temperature in terms of the interionic interaction. The general image that is put forward by these studies is that the ionic mobilities, which largely relate to the electrical conductivity values, are strongly influenced by the exact nature of the interaction between anions and cations. This interaction is built up from the Coulombic interaction between the charges of the ions and the van der Waals interaction between the induced charges in the ions. The exact nature of this interaction then depends on properties such as the structure of the ions, their polarizability, and the possibilities for hydrogen bonding. However, a full understanding of these interactions is not yet achieved.

In this paper, dielectric spectra of different ionic liquids are determined and by properly taking into account the effect of electrode polarization, the temperature dependence of their dc conductivity values is extracted. In comparison with the works cited above, we extend the conductivity curves to much lower temperatures, attaining values close to the glass transition temperatures. In particular, we investigate the dependence of the glass transition temperature (values obtained from the VFT curves and confirmed by DSC measurements), the dynamic fragility, and other parameters derived from the VFT curves on the alkyl chain length of the homologous

---

[a] Electronic mail: jan.leys@fys.kuleuven.be.

series of 1-alkyl-3-methylimidazolium tetrafluoroborate ionic liquids, $[C_n\text{mim}][BF_4]$, where $n=2-11$. In order to determine the influence of the anion on the glass formation, a series of 1-hexyl-3-methylimidazolium ionic liquids with different anions are investigated as well. The anions are bromide Br^-, tetrafluoroborate $[BF_4]^-$, bis(trifluoromethylsulfonyl)imide $[Tf_2N]^-$, and tris(pentafluoroethyl)trifluorophosphate $[FAP]^-$.

II. EXPERIMENTS

The 1-alkyl-3-methylimidazolium tetrafluoroborate ionic liquids $[C_n\text{mim}][BF_4]$ with an even number of carbon atoms in the alkyl chain ($n=2$, 4, 6, 8, and 10) were purchased from IoLiTec (Ionic Liquid Technologies, Germany), whereas those with an odd number of carbon atoms ($n=3$, 5, 7, 9, and 11) were synthesized by a metathesis reaction between the corresponding bromide ionic liquid and sodium tetrafluoroborate in acetone. After filtration, the acetone was removed on a rotary evaporator. The product was then again dissolved in dry acetone and stored for 12 h in a freezer at −20 °C. All precipitates were removed after that by filtration. After removing the acetone by evaporation, the ionic liquids were dried under vacuum at 80 °C on the rotary evaporator. 1-hexyl-3-methylimidazolium bromide, $[C_6\text{mim}]Br$, and bis-(trifluoromethylsulfonyl)imide, $[C_6\text{mim}][Tf_2N]$, were prepared as described in the literature.[9] 1-hexyl-3-methylimidazolium tris(pentafluoroethyl)trifluorophosphate, $[C_6\text{mim}][FAP]$, was provided by Merck (Darmstadt, Germany). The structures of the more complex ions are shown in the inset of Fig. 4.

We did not perform additional purification steps before the measurement for the commercially obtained compounds. The ILs were taken out of the bottle and immediately transferred to the sealed measurement cell, with practically no exposure to air. Since the bottles were not opened before, factory values for purities applied. For the other compounds, water content and halide content were determined. The values have been summarized in Table I.

The halide content of the in-house prepared samples was tested by the silver nitrate test. An aliquot of the ionic liquid was mixed with water and some drops of a $0.1M$ $AgNO_3$ solution were added. None of the samples gave a positive test, corresponding to a halide content below 200 ppm.

For the water content, we do not have the actual values at the time of the measurement, and Karl-Fisher titration was performed only several months after the measurement. For the IL that we synthesized ourselves, we performed first a titration on the IL as it was found in the bottle. After that, we dried these ILs in the same way as they were dried after synthesis and performed again a titration. Comparison indicates that the ILs took up a (mostly limited) amount of water during storage after the measurement. However, the measurements took place shortly after synthesis and drying, which makes us conclude that the water content at the time of the measurements was below 1000 ppm and probably even lower, close to the values we give here for titration after drying. For the other ILs, the titration shows that they did not take up any important amount of water compared to the mea-

TABLE I. Purity-related data for the ionic liquids used in this work.

Compound	Material	Amount	Method	Data source
$[C_2\text{mim}][BF_4]$	Assay	>99%	NMR[a]	Iolitec
	$[C_2\text{mim}]$	99.5%	IC[b]	Iolitec
	$[BF_4]$	99.3%	IC	Iolitec
	Halides	0.4%	IC	Iolitec
	Water	180 ppm	KF[c]	Iolitec
$[C_3\text{mim}][BF_4]$	Halides	<200 ppm	SNT[d]	
	Water	16 064 ppm	KF	
		125 ppm	KF	(after drying)
$[C_4\text{mim}][BF_4]$	Assay	>99%	NMR	Iolitec
	$[C_4\text{mim}]$	99.8%	IC	Iolitec
	$[BF_4]$	99.9%	IC	Iolitec
	Halides	90 ppm	IC	Iolitec
	Water	150 ppm	KF	Iolitec
		131 ppm	KF	
$[C_5\text{mim}][BF_4]$	Halides	<200 ppm	SNT	
	Water	1287 ppm	KF	
		81 ppm	KF	(after drying)
$[C_6\text{mim}][BF_4]$	Assay	>99%	NMR	Iolitec
	$[C_6\text{mim}]$	99.4%	IC	Iolitec
	$[BF_4]$	99.9%	IC	Iolitec
	Halides	70 ppm	IC	Iolitec
	Water	90 ppm	KF	Iolitec
		91 ppm	KF	
$[C_7\text{mim}][BF_4]$	Halides	<200 ppm	SNT	
	Water	1140 ppm	KF	
		139 ppm	KF	(after drying)
$[C_8\text{mim}][BF_4]$	Assay	>99%	NMR	Iolitec
	$[C_8\text{mim}]$	99.7%	IC	Iolitec
	$[BF_4]$	99.9%	IC	Iolitec
	Halides	70 ppm	IC	Iolitec
	Water	110 ppm	KF	Iolitec
$[C_9\text{mim}][BF_4]$	Halides	<200 ppm	SNT	
	Water	1855 ppm	KF	
		135 ppm	KF	(after drying)
$[C_{10}\text{mim}][BF_4]$	Assay	>99%	NMR	Iolitec
	$[C_{10}\text{mim}]$	99.4%	IC	Iolitec
	$[BF_4]$	99.9%	IC	Iolitec
	Halides	80 ppm	IC	Iolitec
	Water	130 ppm	KF	Iolitec
$[C_{11}\text{mim}][BF_4]$	Halides	<200 ppm	SNT	
	Water	1307 ppm	KF	
		150 ppm	KF	(after drying)
$[C_6\text{mim}]Br$	Halides	<200 ppm	SNT	
	Water	14 880 ppm	KF	
		163 ppm	KF	(after drying)
$[C_6\text{mim}][Tf_2N]$	Halides	<200 ppm	SNT	
	Water	1335 ppm	KF	
		66 ppm	KF	(after drying)
$[C_6\text{mim}][FAP]$	Halides	<200 ppm	SNT	
	Water	168 ppm	KF	

[a] Nuclear magnetic resonance spectroscopy.
[b] Ion chromatography.
[c] Karl-Fisher titration.
[d] Silver nitrate test, see text for a description.

surement results provided by the supplier, indicating that these supplier values still applied at the time of measurement.

The thermal stability of the samples during the measurement was *a priori* not considered as a problem, since the used ILs are known to be rather stable and the temperature range was limited to 120 °C. The samples were visually inspected after measurement for color changes that might indicate decomposition; however, no color change or other effect of degradation was noticed.

Dielectric measurements were performed by a Novocontrol Alpha analyzer in combination with a Novocontrol Quatro temperature controller. The sample was placed in a sealed stainless steel parallel plate capacitor of 17 mm diameter and 0.5 mm thickness. The data were analyzed in terms of the dielectric permittivity $\epsilon^* = \epsilon' - i\epsilon''$, from which the imaginary part gives the conductivity σ, as for pure Ohmic conduction $\epsilon'' = \sigma/(\epsilon_0 \omega)$, with ϵ_0 the permittivity of vacuum and ω the angular frequency of the applied electric field. For the data analysis, those regions in the measured ϵ'' were selected where the slope of log ϵ'' versus log ω was -1 ± 0.02. Then, the values of σ were determined locally and finally, these numbers were averaged, resulting in the σ values presented in this work.

This approach is in contrast to most other dielectric works in the literature. Several works have been devoted to the determination of the static value of the dielectric permittivity;[10–15] however, this requires much higher measuring frequencies than used in this work. Some researchers have also performed dielectric work in the same frequency range, but they have interpreted their results mainly in terms of the dielectric modulus[16–18] or focused on β relaxations.[19]

Glass transition temperatures (T_g) were obtained from a standard DSC experiment. Aluminum sample holders were placed in a Q1000 from TA Instruments. The glass transition temperature was determined as the value of the inflection point of the heat flow determined in a 10 K/min heating run.

III. RESULTS AND DISCUSSION

In Fig. 1, the real and imaginary parts of the complex permittivity of $[C_7mim][BF_4]$ as a function of frequency at 248.15 K are presented. The high frequency part of ϵ'', indicated by Cond in the figure, is the part of the spectrum dominated by the dc conductivity, showing as a straight line with slope of -1. At lower frequencies, a shoulder is present, after which again a linear behavior is visible, at a slope of less than -1. The real part is dominated by electrode polarization below about 2 kHz, indicated by EP. The strong increase flats off after the peak in the imaginary part, and a region starts where the phase angle is nearly constant (CPA). The inset shows the frequency dependence of the conductivity. In this representation, three regions can be identified: The region of electrode polarization (EP), the region where the dc conductivity should be determined (Cond), and the region of subdiffusive conductivity (SD).[20,21] This is a prototype spectrum for all $[C_nmim][BF_4]$ ILs at these temperatures and up to 393 K. The increase in ϵ' caused by the electrode polarization and the corresponding peak in ϵ'' shift to higher frequencies with increasing temperatures; the later lies typically at around 100 kHz at room temperature.

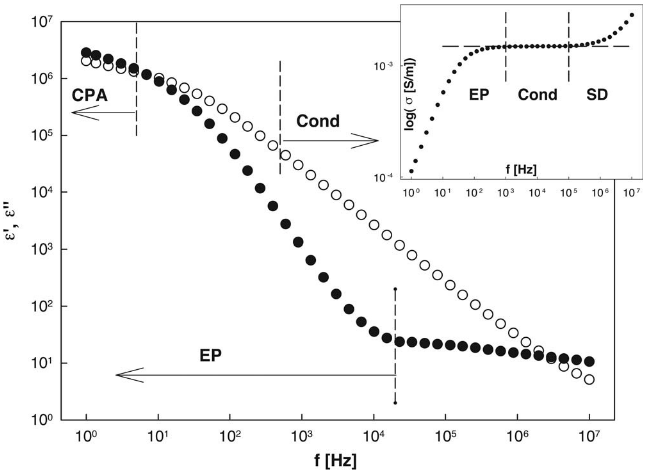

FIG. 1. Real (●) and imaginary (○) parts of the complex permittivity of $[C_7mim][BF_4]$ as a function of the frequency at 248.15 K. Inset: The conductivity as a function of frequency. See text for the meanings of the abbreviations.

For comparison, we have compiled in Table II a number of literature values for the electrical conductivity of different compounds included in this study. In general, our values are consistent with those given in the literature. Small deviations can be explained as follows. Since the conductivity values are sensitive to temperature variations, differences in thermometers or temperature stabilization may already explain part of the difference. Also, small uncertainties in the cell constant (or in our case, the geometry of the parallel plate capacitor) can be responsible. We should point out that our measurement technique and data analysis procedure are quite similar to the standard approaches used for conductivity determination. We determine the magnitude and phase angle of the impedance of the ionic liquid over a broad frequency range and calculate directly from these values the real and imaginary parts of the dielectric permittivity. The advantage of this alternative representation of the impedance data is that the regions where the conductivity should be determined are directly visible, as is the influence of the electrode polarization. In fact, determination of the conductivity by fitting a straight line through the imaginary part of the dielectric permittivity is easier than, for example, a determination based on a Nyquist plot of the impedance, where an extrapolation has to be made.[4]

In Fig. 2, an overview of the conductivity values obtained for all the $[C_nmim][BF_4]$ ILs as a function of temperature is shown. The values of σ decrease with increasing chain length. As the conductivity is related to the mobility of the charge carriers, this can be explained by the higher viscosity induced by the stronger van der Waals interactions between the longer alkyl chains and by the larger cation size. Also, a longer alkyl chain results in a larger volume fraction of the neutral hydrocarbon part of the organic cation.

It appears that the $[C_nmim][BF_4]$ ILs are glassforming systems. Therefore, the conductivity data were fitted to the empirical VFT equation, which usually describes the tem-

TABLE II. Comparison of the conductivity values for a number of the studied ionic liquids at different temperatures.

Compound	T (K)	σ (S/m) This work	σ (S/m) Literature	Reference
$[C_2mim][BF_4]$	258.15	0.24	0.25	7
	278.15	0.72	0.74	7
	293.15	1.3		
	295.15		1.2	25
	298.15	1.5	1.6	7
			1.4	26
			1.4	27
			1.4	22
	299.15		1.3	28
	303.15	1.7	2.0	29
	333.15	3.9	3.6	7
	393.15	9.0	8.8	7
	RT[a]		1.6	31
$[C_3mim][BF_4]$	298.15	0.65	0.59	22
$[C_4mim][BF_4]$	273.15	0.09	0.033	30
	293.15	0.36		
	294.5		0.15	30
	298.15	0.46	0.35	22
	303.15	0.58	0.35	23
	333.5	1.6	0.88	30
	RT		0.35	31
$[C_6mim][BF_4]$	293.15	0.12		
	298.15	0.16		
	RT		0.12	31
$[C_6mim][Tf_2N]$	288.15	0.132	0.135	24
	293.15	0.169	0.173	24
	298.15	0.212	0.218	24
	308.15	0.310	0.327	24

[a] Room temperature. No explicit temperature value given.

perature dependence of the structural relaxation time and the electrical conductivity of supercooled liquids quite well. It also allows us to obtain information about the fragility of these systems and other parameters related to glassy behavior. The results of the fitting are summarized in Table III. The VFT law has been fitted through the data points in its linearized form

$$\ln \sigma = \ln \sigma_\infty - \frac{B}{T - T_0}, \tag{1}$$

where B describes the temperature dependence of σ in the high temperature limit and T_0 is the Vogel temperature.

The determination of the fragility m, which is calculated by[32]

$$m = \frac{B}{2.303} \frac{T_g}{(T_g - T_0)^2}, \tag{2}$$

requires in this form not only the knowledge of the VFT fit parameters but also of the glass transition temperature T_g. In the case of dielectric relaxation times, it is a common practice to define T_g as the temperature at which the relaxation time is 100 s. However, to our knowledge, there exists no such criterion for the conductivity values. Nevertheless, we have used an *ad hoc* value of $\sigma(T_g) = 10^{-12}$ S/m to extract a glass transition temperature T_g^σ from the conductivity data. The validity of our definition for the samples under investigation is confirmed by Fig. 3, in which the extracted T_g^σ values are compared with values T_g^{DSC} obtained by DSC measurements.

This value $\sigma(T_g) = 10^{-12}$ S/m should be considered as an *ad hoc* value for the $[C_nmim][BF_4]$ series. It will, for example, not be correct for the case of $[C_6mim]Br$. We think that future work might show that the value proposed here is, in fact, a translation of a rule of thumb for the orientational relaxation times, which states that $\tau(T_g) \approx 10^{-16}\tau_\infty$, where τ_∞ is the high temperature limit of the relaxation time, i.e., the prefactor in the VFT law. τ_∞ typically takes values of around 10^{-13} s, and this results then in the value of 100 s for $\tau(T_g)$ cited above. It is not unlikely that a corresponding relationship can be established for the relation between $\sigma(T_g)$ and σ_∞; however, we would like to acquire a broader data set to make such analysis.

The value for T_g^σ has been used for the calculation of the data points in the inset of Fig. 2. The fragility m itself is presented in the inset of Fig. 3. These values were calculated with Eq. (2) while using T_g^{DSC}. Since $[C_2mim][BF_4]$ could not be fitted with a single VFT expression and since $[C_{10}mim][BF_4]$ and $[C_{11}mim][BF_4]$ crystallized, no values for the fragility are given for those three compounds.

The VFT parameters show some interesting dependences on the alkyl chain length. First of all, if we look at the values of the prefactor σ_∞, we see that the decreasing trend in the room temperature electrical conductivity is also reflected in the decreasing values of this parameter. The values of B are globally increasing with the chain length. This is essentially the same trend as the decreasing fragility with chain length and will be discussed below. The Vogel temperatures T_0 for the $[C_nmim][BF_4]$ ILs are rather constant at around 147 K. However, these trends break down for $[C_{10}mim][BF_4]$ and $[C_{11}mim][BF_4]$. This is a consequence of the crystallization of these compounds, as it means that the data set over which we fit the VFT law is seriously limited and lies at higher temperatures than for the other compounds. For the other series, $[C_6mim]^+$ with different anions, $[BF_4]^-$, $[Tf_2N]^-$, and $[FAP]^-$, show comparable values, whereas Br^- shows larger B and T_0 values.

The tendencies that we found for $n=2-9$ break down for $n=10$ and 11. The increasing length of the alkyl chain apparently favors crystallization over supercooling and glass formation. This may be explained by the higher mobility of the shorter alkyl chain; however, such discussion is outside the scope of this paper.

Since the behavior of all investigated ILs (except for $[C_2mim][BF_4]$) in this homologous series can be fitted with a single VFT curve, all compounds can be well characterized by a limited set of parameters, i.e., the VFT parameters σ_∞, B, and T_0, which allow the determination of T_g and m. Xu *et al.*[8] have already discussed in detail the influence on the VFT behavior of the IL anion. In their analysis, while interpreting Walden's rule and the Debye-Einstein relation to link electrical conductivity to molecular diffusivity and viscosity, the

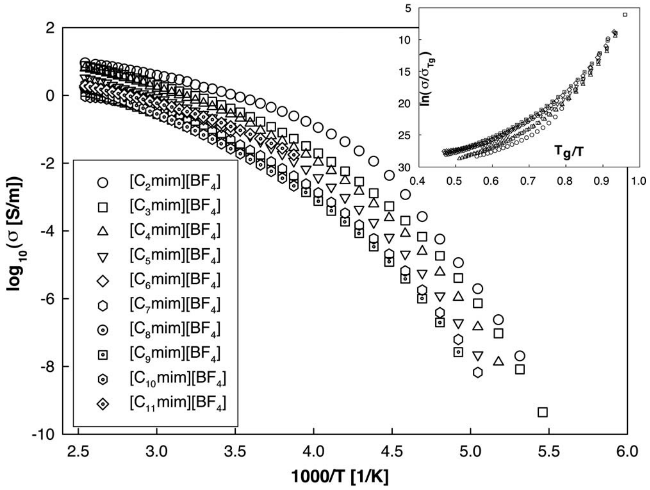

FIG. 2. Conductivity values of $[C_n\mathrm{mim}][BF_4]$ as a function of the inverse temperature. Inset: The same data rescaled, presented as $\ln(\sigma/\sigma_{T_g})$ vs T_g/T.

value of T_g was associated with the cohesive force between the ions, which turns out to be mainly determined by the molecular volume. At low molecular (or equivalently, molar) volumes, this force is dominated by attractive Coulomb forces between ions, which decreases with increasing molar volume. At larger molar volumes ($>250\ \mathrm{cm^3/mol}$), van der Waals forces start to dominate, leading to an increasing value of T_g with molar volume. The series of samples investigated here, where the molar volume of the slowest ion (and, thus, most important for the overall ionic diffusivity) increases with the increasing length of the alkyl chain attached to the cation, can be situated in the latter range and indeed follows the earlier observed trend of significantly increasing T_g values. Thus, via the influence on cohesive forces and the value of T_g, in the van der Waals regime, the alkyl chain plays an important role in the molecular mobility and, thus, electrical conductivity. On the other hand, the homologous series shows a quite weak decrease of fragility with increasing alkyl chain length. The fragility values lie at around 70, which is an intermediate value compared with other glass formers. The relation between molecular parameters and fragility is not yet well understood. However, it is known for ILs that the fragility, which is closely connected with the morphology of the energy landscape and cooperativity of network rearrangements,[33] depends very strongly[8] on local interionic Coulomb forces. In this case, these dominantly occur between the small BF_4 anion and the imidazolium part of the cation and are thus only indirectly influenced by the alkyl chain. The relation found here between fragility and T_g goes somehow against the increasing trend observed by Qin *et al.*[34] for organic ionic glasses, which was, however, quite scattered.

To verify how important the influence of the anion is on the fragility, we also studied a short series of ionic liquids in which different anions were combined with a $[C_6\mathrm{mim}]^+$ cation. In the series, the anion size increases from a single bromide to the large $[\mathrm{FAP}]^-$ ion. The results are presented in Fig. 4 and in Table III. The room temperature conductivity values and the fragility for $[C_6\mathrm{mim}][BF_4]$, $[C_6\mathrm{mim}][Tf_2N]$, and $[C_6\mathrm{mim}][\mathrm{FAP}]$ are quite alike, while the significantly lower conductivity value and the significantly higher value of the fragility for $[C_6\mathrm{mim}]Br$ are an exception in this series.

The fragility of the ionic liquid $[C_6\mathrm{mim}]Br$ is much larger than the fragility of the ionic liquids with fluorinated anions. This anomaly can be explained by the fact that the bromide ion is able to form strong hydrogen bonds with the hydrogen atoms of the imidazolium cation.[35,36] The interionic forces lead to the formation of a hydrogen-bonded network and, thus, to a higher fragility. The presence of this network also makes it more difficult for the ions to move through the sample, causing the much lower conductivity. The fluorinated anions have a lower charge density because the negative charge is spread over a much large volume. The interaction of these anions with the imidazolium cation is much weaker than the interaction between the bromide anion

TABLE III. VFT fitting parameters and derived quantities for the ionic liquids in this work.

	σ_{RT}[a]	T_g	$\ln \sigma_\infty$	B	T_0	m
$[C_2\mathrm{mim}][BF_4]$[b]	1.282	172.0	⋯	⋯	⋯	⋯
$[C_3\mathrm{mim}][BF_4]$	0.519	175.1	7.86	1284	139.7	78
$[C_4\mathrm{mim}][BF_4]$	0.364	177.9	6.89	1160	146.8	93
$[C_5\mathrm{mim}][BF_4]$	0.163	182.8	6.69	1240	147.1	78
$[C_6\mathrm{mim}][BF_4]$	0.118	187.6	6.37	1238	148.5	66
$[C_7\mathrm{mim}][BF_4]$	0.067	186.1	6.03	1291	146.1	68
$[C_8\mathrm{mim}][BF_4]$	0.059	189.7	6.10	1295	148.3	62
$[C_9\mathrm{mim}][BF_4]$	0.042	190.5	5.80	1324	145.9	55
$[C_{10}\mathrm{mim}][BF_4]$[c]	0.037	⋯	7.26	1750	127.4	⋯
$[C_{11}\mathrm{mim}][BF_4]$[d]	0.154	⋯	3.77	716	166.3	⋯
$[C_6\mathrm{mim}]Br$	0.0074	187.8	7.47	1668	158.4	158
$[C_6\mathrm{mim}][Tf_2N]$	0.170	187.1	5.59	1057	148.3	57
$[C_6\mathrm{mim}][\mathrm{FAP}]$[e]	0.096	184.7	3.86	965	152.2	73

[a] The value for σ at room temperature, $T=293.15$ K, expressed in S/m.

[b] As can be seen from the figure, $[C_2\mathrm{mim}][BF_4]$ cannot be fitted with a single VFT expression; therefore, no parameters are quoted.

[c] $[C_{10}\mathrm{mim}][BF_4]$ crystallizes at about 248–258 K. There was no glass transition found.

[d] $[C_{11}\mathrm{mim}][BF_4]$ crystallizes at about 248 K. There was no glass transition found.

[e] VFT fit has been performed over a very limited data range.

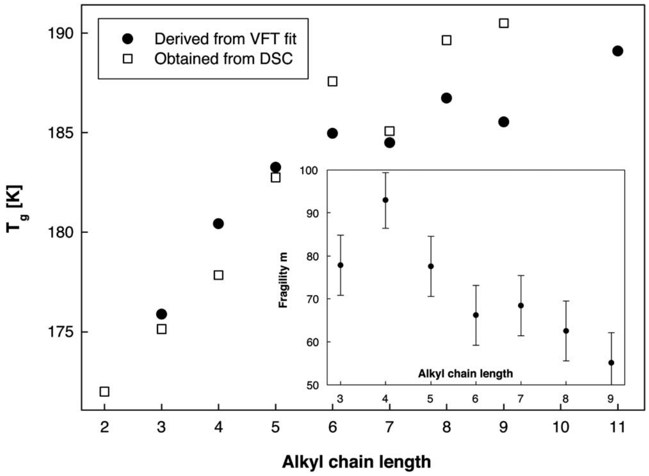

FIG. 3. Glass transition temperatures as a function of alkyl chain length, obtained from DSC experiments (□) compared with those calculated from VFT parameters by choosing $\sigma(T_g)=10^{-12}$ S/m (●). Inset: Fragility values of 1-alkyl-3-methylimidazolium tetrafluoroborates as a function of the alkyl chain length.

and the cation. The results also suggest that $[C_n\text{mim}][\text{FAP}]$ ILs, with $n=1$, 2, and 3, could be good candidates for a high room temperature electrical conductivity. In view of the technological interest in such ILs, we will also investigate multivalent ions in the future.

IV. CONCLUSION

We have studied the glassforming behavior of two series of ionic liquids, namely, the 1-alkyl-3-methylimidazolium tetrafluoroborate ionic liquids with varying chain length and the 1-hexyl-3-methylimidazolium ionic liquids with varying anion, by an analysis of the electrical conductivity of these systems.

The glass transition temperatures increase with increasing alkyl chain length in the first series; until for $n=10$, the glass transition is replaced by a crystallization. Analysis of the electrical conductivity values and their VFT fits shows a decreasing conductivity with chain length, reflecting reduced mobility of the ions. The value of T_0 is rather constant in this series. The B fitting parameters show an increase with chain length. In the series with varying anion, glass transition temperatures are rather constant. Most parameters are comparable for the different compounds, except for 1-hexyl-3-methylimidazolium bromide.

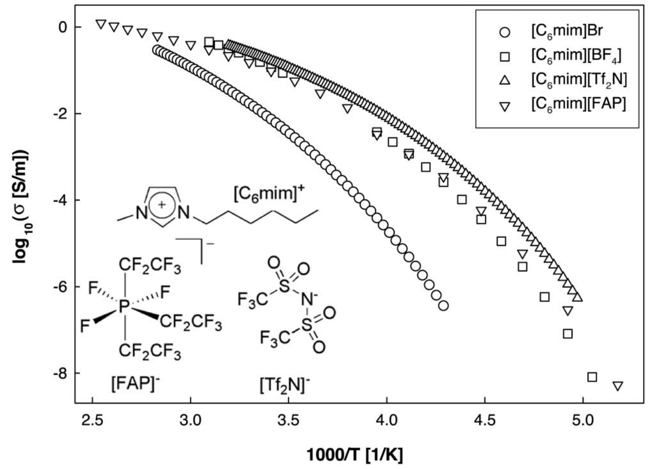

FIG. 4. Conductivity as a function of the inverse temperature for a series of 1-hexyl-3-methylimidazolium ionic liquids. Inset: Structure of the 1-hexyl-3-methylimidazolium cation $[C_6\text{mim}]^+$ and of the $[\text{FAP}]^-$ and $[\text{Tf}_2\text{N}]^-$ anions.

In the series with varying chain length, we observe a decreasing fragility with chain length, which can be understood from the fact that the van der Waals forces between the molecules increase with chain length. The variation of the fragility in the series with varying anion is rather limited, except for 1-hexyl-3-methylimidazolium bromide, where the presence of hydrogen bonds changes the interionic interaction and also the fragility.

ACKNOWLEDGMENTS

Research was supported by IDO/05/005, “Ionic liquids as medium for catalytic reactions and electrodeposition of metal layers,” K.U. Leuven, by Tournesol Exchange Project No. T2006.05 between K.U. Leuven, Belgium and Université du Littoral, Dunkerque, France, by FWO-V, Belgium, Project No. G.0230.07 (“AVISCO”), and by GOA/2007/06/ Project, K.U. Leuven. J.L. acknowledges the Research Fund of K.U. Leuven for a postdoctoral fellowship (No. PDM/07/098). The authors thank Merck (Darmstadt, Germany) for the kind gift of the $[\text{FAP}]^-$ ionic liquid.

[1] K. R. J. Seddon, J. Chem. Technol. Biotechnol. **68**, 351 (1997).
[2] T. Welton, Chem. Rev. (Washington, D.C.) **99**, 2071 (1999).
[3] P. Wasserscheid and W. Keim, Angew. Chem., Int. Ed. **39**, 3773 (2000).
[4] P. Wasserscheid and T. Welton, *Ionic Liquids in Synthesis* (Wiley-VCH, Weinheim, 2002).
[5] H. Tokuda, K. Hayamizu, K. Ishii, Md. A. B. H. Susan, and M. Watanabe, J. Phys. Chem. B **108**, 16593 (2004).
[6] H. Tokuda, K. Hayamizu, K. Ishii, Md. A. B. H. Susan, and M. Watanabe, J. Phys. Chem. B **109**, 6103 (2005).
[7] J. Vila, P. Ginés, J. M. Pico, C. Franjo, E. Jiménez, L. M. Varela, and O. Cabeza, Fluid Phase Equilib. **242**, 141 (2006).
[8] W. Xu, E. I. Cooper, and C. A. Angell, J. Phys. Chem. B **107**, 6170 (2003).
[9] P. Nockemann, K. Binnemans, and K. Driesen, Chem. Phys. Lett. **415**, 131 (2005).
[10] K. Yamamoto, M. Tani, and M. Hangyo, J. Phys. Chem. B **111**, 4854 (2007).
[11] H. Weingärtner, Z. Phys. Chem. **220**, 1395 (2006).
[12] C. Wakai, A. Oleinikova, M. Ott, and H. Weingärtner, J. Phys. Chem. B **109**, 17028 (2005).
[13] H. Weingärtner, P. Sasisanker, C. Daguenet, P. J. Dyson, I. Krossing, J. M. Slattery, and T. Schubert, J. Phys. Chem. B **111**, 4775 (2007).
[14] C. Daguenet, P. J. Dyson, I. Krossing, A. Oleinikova, J. Slattery, C. Wakai, and H. Weingärtner, J. Phys. Chem. B **110**, 12682 (2006).
[15] S. Schrödle, G. Annat, D. R. MacFarlane, M. Forsyth, R. Buchner, and G. Hefter, Chem. Commun. (Cambridge) **2006**, 1748.
[16] N. Ito, W. Huang, and R. Richert, J. Phys. Chem. B **110**, 4371 (2006).
[17] N. Ito and R. Richert, J. Phys. Chem. B **111**, 5016 (2007).
[18] A. Rivera, A. Brodin, A. Pugachev, and E. A. Rössler, J. Chem. Phys. **126**, 114503 (2007).
[19] A. Rivera and E. A. Rössler, Phys. Rev. B **73**, 212201 (2006).
[20] J. C. Dyre and T. B. Schrøder, Rev. Mod. Phys. **72**, 873 (2000).
[21] B. Roling, C. Martiny, and S. Brückner, Phys. Rev. B **63**, 214203 (2001).
[22] T. Nishida, Y. Tashiro, and M. Yamamoto, J. Fluorine Chem. **120**, 135 (2003).
[23] H. Tokuda, S. Tsuzuki, Md. A. B. H. Susan, K. Hayamizu, and M. Watanabe, J. Phys. Chem. B **110**, 19593 (2006).
[24] J. A. Widegren, E. M. Saurer, K. N. Marsh, and J. W. Magee, J. Chem. Thermodyn. **37**, 569 (2005).
[25] T. E. Sutto, H. C. De Long, and P. C. Trulove, *Progress in Molten Salt*

Chemistry, edited by R. W. Berg and H. A. Hjuler (Elsevier, Paris, 2000), Vol. 1, p. 511.

[26] J. Fuller, R. T. Carlin, and R. A. Osteryoung, J. Electrochem. Soc. **144**, 3881 (1997); J. Fuller, R. A. Osteryoung, and R. T. Carlin, Abstracts of Papers, 187th Meeting of The Electrochemical Society, Reno, NV, 1995 (unpublished), Vol. 95-1, p. 27.

[27] A. Noda, K. Hayamizu, and M. Watanabe, J. Phys. Chem. B **105**, 4603 (2001).

[28] A. B. McEwen, H. L. Ngo, K. LeCompte, and J. L. Goldman, J. Electrochem. Soc. **146**, 1687 (1999).

[29] A. Noda and M. Watanabe, Electrochim. Acta **45**, 1265 (2000).

[30] P. A. Z. Suarez, S. Einloft, J. E. L. Dullius, R. F. de Souza, and J. Dupont, J. Chim. Phys. Phys.-Chim. Biol. **95**, 1626 (1998).

[31] For values from the online catalog of Solvent Innovation. See http://www.solvent-innovation.com/.

[32] R. Böhmer, K. L. Ngai, C. A. Angell, and D. J. Plazek, J. Chem. Phys. **99**, 4201 (1993).

[33] P. G. Debenedetti and F. H. Stillinger, Nature (London) **410**, 259 (2001).

[34] Q. Qin and G. B. McKenna, J. Non-Cryst. Solids **352**, 2977 (2006).

[35] A. G. Avent, P. A. Chaloner, M. P. Day, K. R. Seddon, and T. Welton, J. Chem. Soc. Dalton Trans., 3405 (1994).

[36] A. Elaiwi, P. B. Hitchcock, K. R. Seddon, N. Srinivasan, Y. M. Tan, T. Welton, and J. A. Zora, J. Chem. Soc. Dalton Trans., 3467 (1995).